Electronic Supplementary Information

Dense π-stacking of flexible ligands fixed in interpenetrating Zn(II) MOF exhibiting long-last phosphorescence and efficient carrier transport

Mei-Li Zhang,[a] Ye Bai,[a] Xiao-Gang Yang,[b]* Yan-Jin Zheng,[a] Yi-Xia Ren,[a] Ji-Jiang Wang,[a] Min-Le Han,[b] Fei-Fei Li,[c] and Lu-Fang Ma[b]*

[a]Department of Chemistry and Chemical Engineering, Yan′an University, Laboratory of New Energy & New Function Materials, Yan′an, Shaanxi 716000, P. R. China.
[b]College of Chemistry and Chemical Engineering, Luoyang Normal University, Henan Key Laboratory of Function-Oriented Porous Materials, Luoyang 471934, P. R. China.
[c]College of Chemistry and Chemical Engineering, Henan Polytechnic University, Jiaozuo, 454000, P. R. China.
E-mail: mazhuxp@126.com

1. Experimental Section

1.1. Materials and methods

All the starting reagents and solvents were commercially available and used as received without further purification. The hydrothermal reaction was performed in a 25 mL Teflon-lined stainless steel autoclave under autogenous pressure. Elemental analyses for C, H, and N were carried out on a Flash 2000 organic elemental analyzer. Thermal gravimetric analyses (TGA) were carried out on a SDT Q600 thermogravimetric analyzer with a heating rate of 10 °C/min under a N_2 atmosphere. Powder X-ray diffraction (PXRD) measurements were performed on a Bruker D8-ADVANCE X-ray diffractometer with Cu Kα radiation (λ = 1.5418 Å). X-ray single-crystal diffraction data for **1** was collected on a Bruker Smart 1000 CCD area-detector diffractometer with Mo-Kα radiation (λ = 0.71073 Å) by ω scan mode. The crystal structure was solved by direct methods, using SHELXS-2014 and least-squares refined with SHELXL-2014 using anisotropic thermal displacement parameters for all non-hydrogen atoms.[1] Further details for structural analysis are summarized in Table S1. The crystallographic data for **1** are listed in Table S1. CCDC No. 1969030 contains the supplementary crystallographic data for **1**. This material can be obtained free of charge via http://www.ccdc.cam.ac.uk/conts/retrieving.html, or from the Cambridge Crystallographic Data Centre, 12 Union Road, Cambridge CB2 1EZ, UK; fax: (+44) 1223-336-033; or E-mail: deposit@ccdc.cam.ac.uk. The solid UV−vis absorption spectra were measured on a Shimadzu UH4150 spectrophotometer. Room temperature photoluminescence (PL) spectra and time-resolved lifetime were

conducted on an Edinburgh FLS1000 fluorescence spectrometer. The fluorescence spectra were measured by a continuous radiation of xenon arc lamp (Xe900). While the phosphorescence spectra and phosphorescence decay curves were tested by a pulsing radiation of microsecond flash lamp with time-resolved single photon counting–multi-channel scaling (MCS) mode. The phosphorescence quantum yield value at room temperature was estimated using a Teflon-lined integrating sphere (F-M101, Edinburgh, diameter: 150 mm and weight: 2 kg) in FLS1000 fluorescence spectrometer.

2. Synthesis of [Zn(mpda)(mbiyb)] (1)

A mixture of H_2mpda (21.0 mg, 0.1 mmol), $Zn(NO_3)_2 \cdot 6H_2O$ (29.7 mg, 0.10 mmol), mbiyb (19.4 mg, 0.1 mmol) and KOH (5.6 mg, 0.1 mmol) were added to water (12 mL) in a 25 mL Teflon-lined stainless steel vessel. The mixture was heated at 160 ºC for 72 h. After the reactive mixture was slowly cooled to room temperature, colourless block crystal of **1** was obtained (yield: 80 %, based on Zn). Elemental analysis calcd. (%) for $C_{24}H_{22}N_4O_4Zn$: C 58.09, H 4.44, N 11.29; found (%): C 57.88, H 4.27, N 11.03.

3. Optoelectronic measurements

Optoelectronic measurements were performed with a CHI 660E electrochemical analyzer (CH Instruments, Chenhua Co., Shanghai, China) in a standard three-electrode system using powder of MOF modified indium tin oxide (ITO) glass as the working electrodes with a working area of 1.0 cm^2, a platinum wire electrode as a counter electrode, Ag/AgCl as a reference electrode, and 0.5 M Na_2SO_4 aqueous

solution as the electrolyte. The system was conducted in a quartz glass reactor ca. 50 cm^3, and irradiated by a 300 W xenon lamp. Transient current density-time characteristics was tested without additional bias potential. Mott–Schottky curve of **1** were performed at an alternating current frequency of 1 kHz under dark conditions.

4. Electronic structure calculations

All calculations were performed with the density functional theory (DFT) method using $Dmol^3$ module in Material Studio software package. The initial configuration was fully optimized by Perdew-Wang (PW91) generalized gradient approximation method with the double numerical basis sets plus polarization function.[2] The core electrons for metals were treated by effective core potentials.

2. Supporting Figures

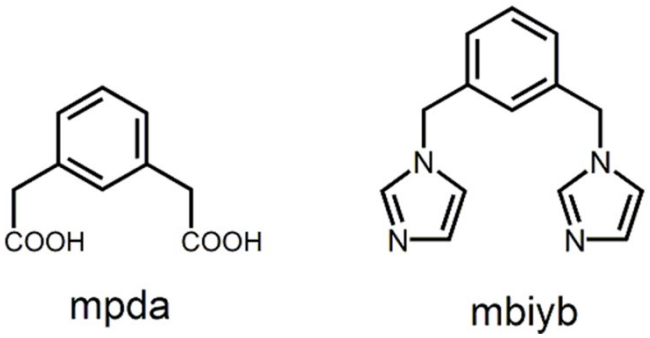

mpda mbiyb

Scheme S1 Chemical structures of 1,3-phenylenediacetic acid (mpda) and 1,3-bis(imidazol-1-ylmethyl)benzene (mbiyb) in this work.

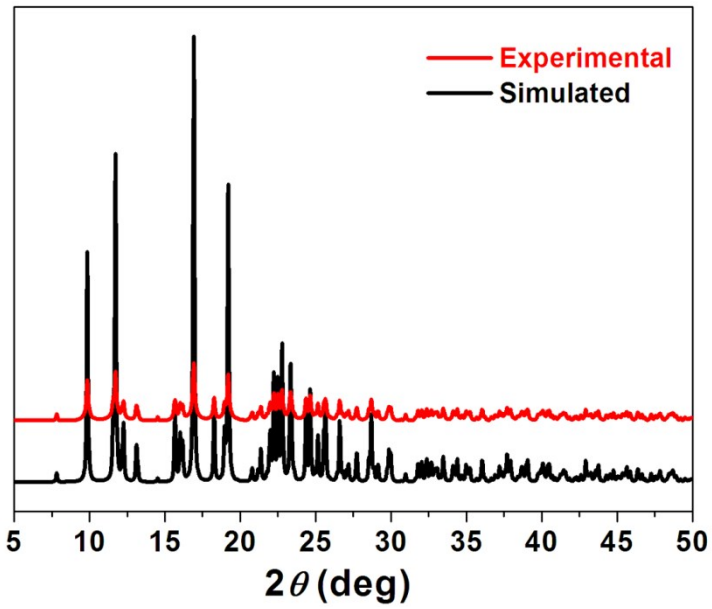

Fig. S1 Experimental (black) and simulated (red) PXRD patterns of **1**.

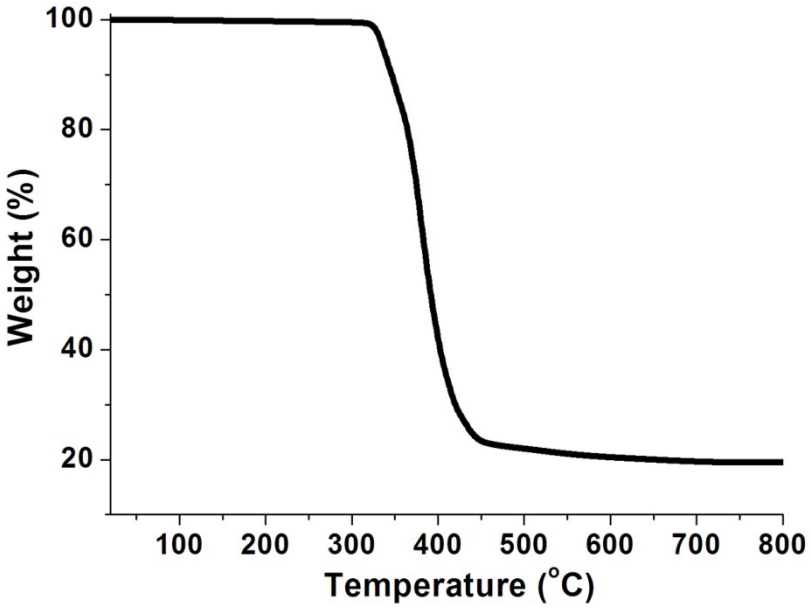

Fig. S2 Thermo gravimetric analysis curve of **1**.

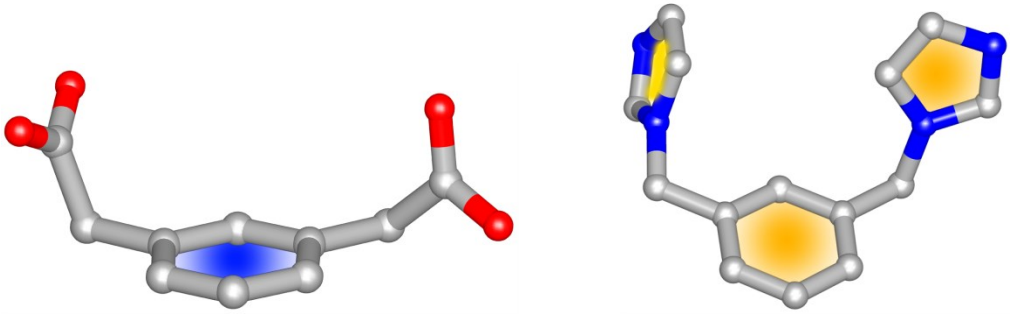

(a) (b)

Fig. S3 View of the conformations of mpda (a) and mbiyb (b) building blocks in **1**.

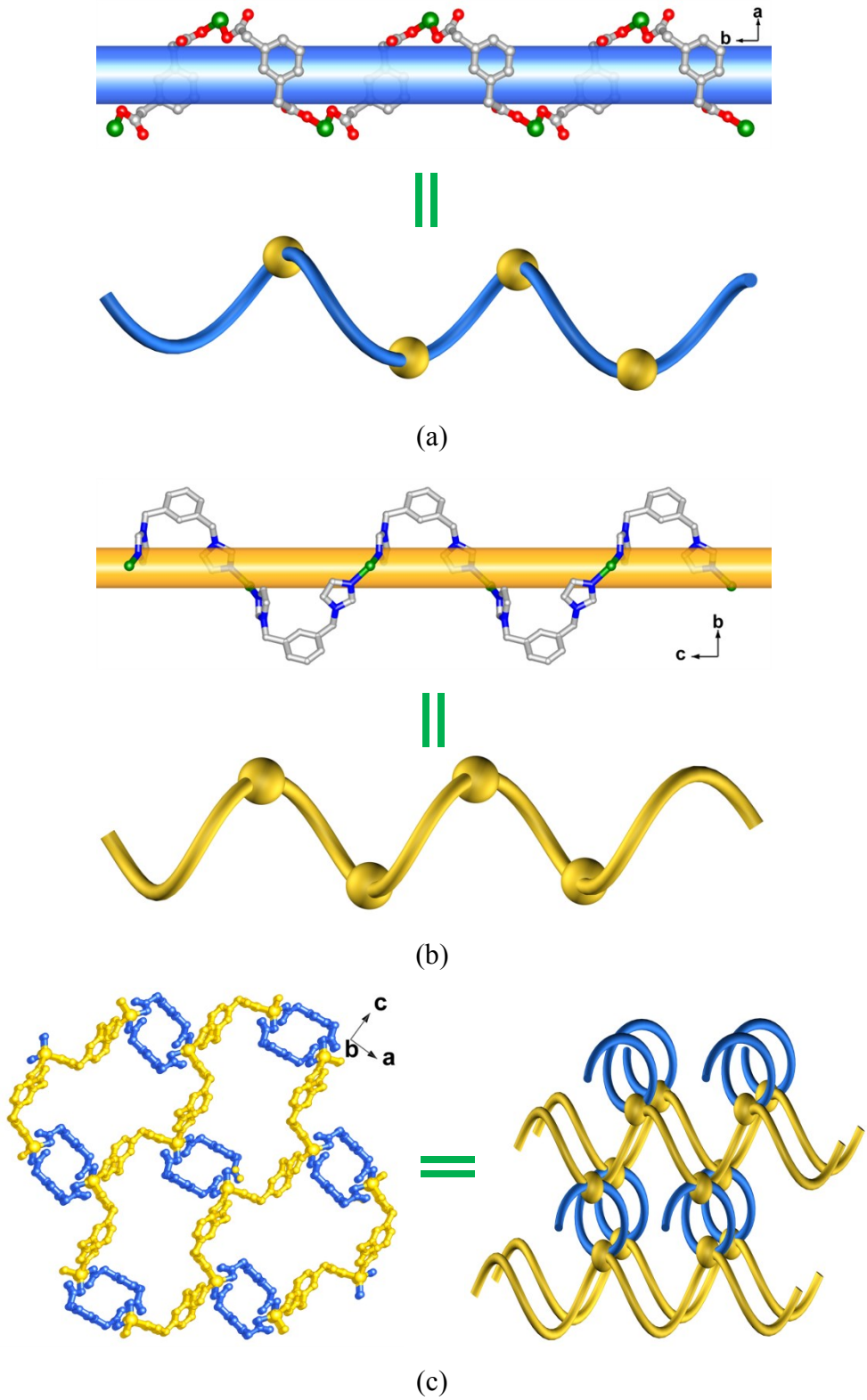

Fig. S4 View of right- and left-handed helixes induced by mpda (a) and mbiyb (b). (c) Two kind of helical chains share the Zn(II) atoms giving rise to the 3D network with the alternate arrangement of right- and left-handed helixes.

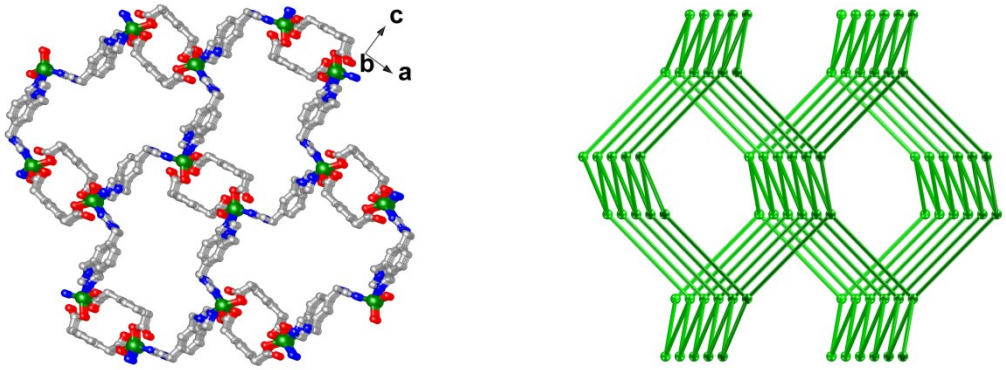

(a)

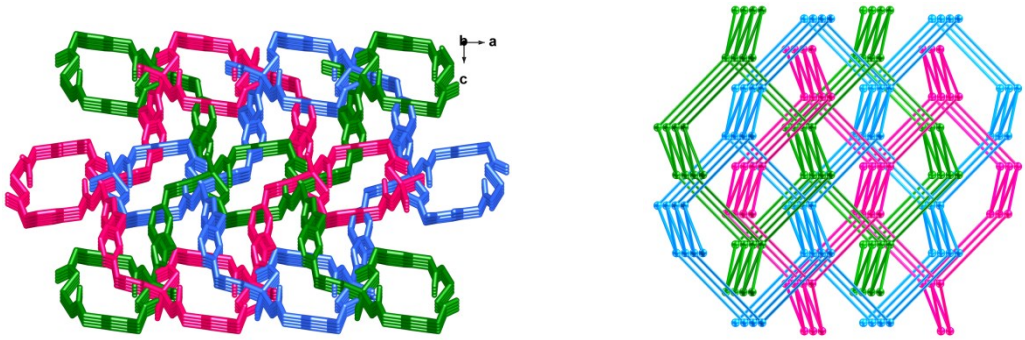

(b)

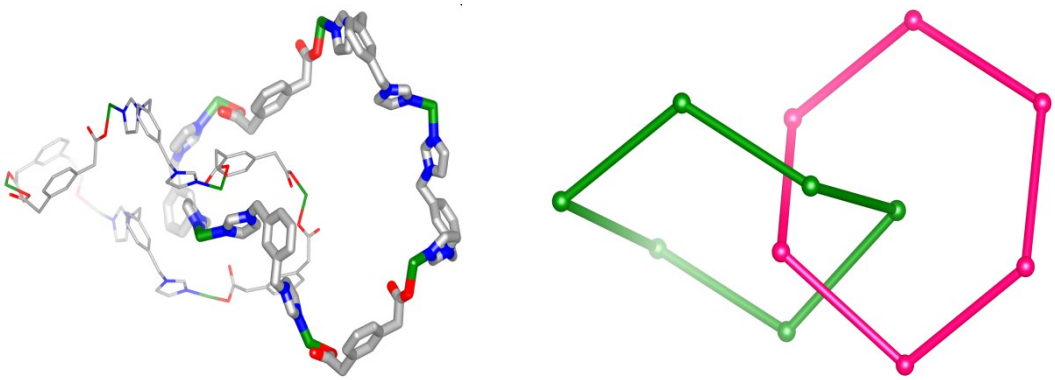

(c)

Fig. S5 Ball-and-stick view (left) and schematic representation (right) of single (a) and 3-fold parallel interpenetrating (b) network of **1**. (Networks show different color for clarity). (c) View of two interpenetrating $[Zn_6(mpda)_2(mbiyb)_4]$ rings.

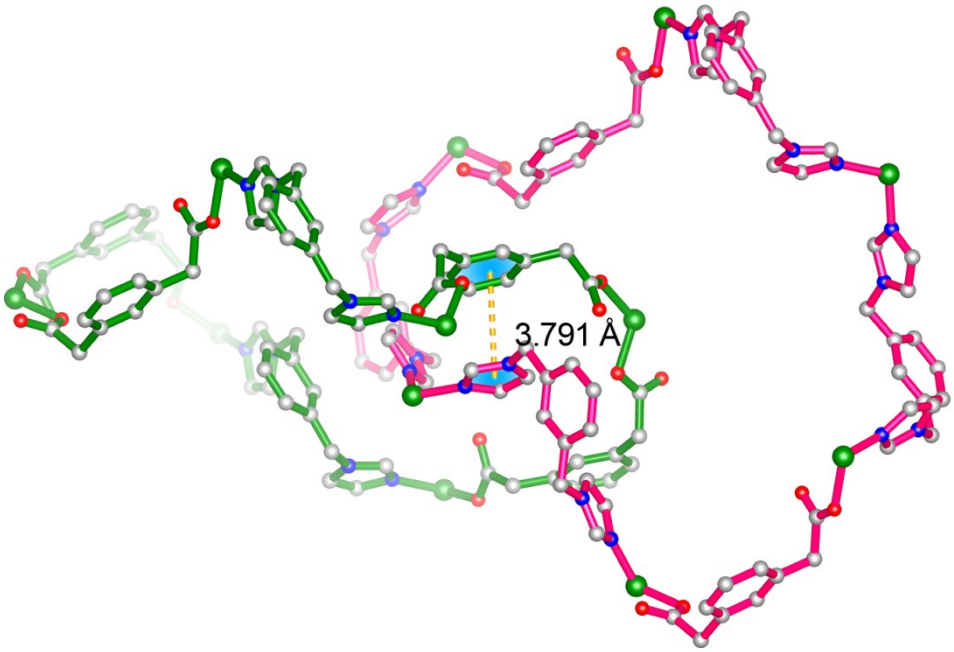

Fig. S6 View of π···π stacking between midazole rings of mbiyb and benzene rings of mpda from different networks.

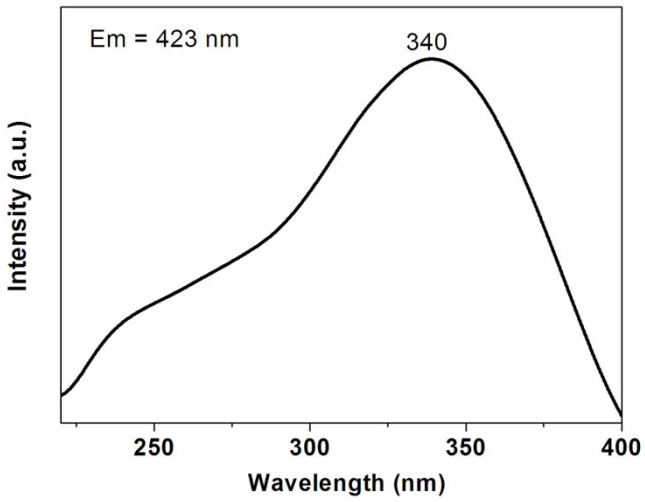

(a)

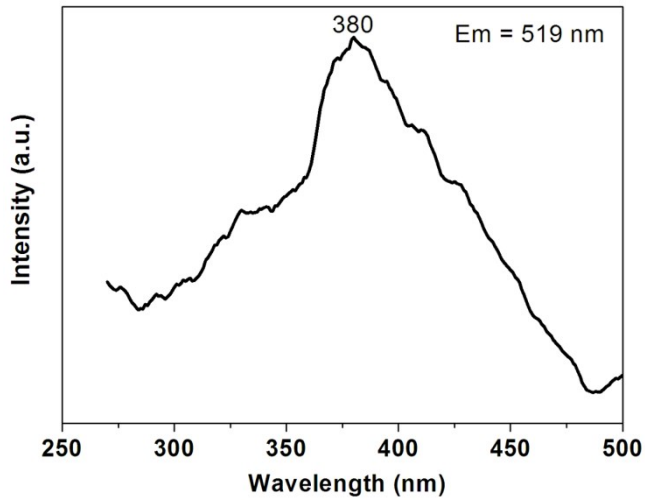

(b)

Fig. S7 The excitation spectra of the fluorescent (a) and phosphorescent (b) bands for **1** measured at room temperature.

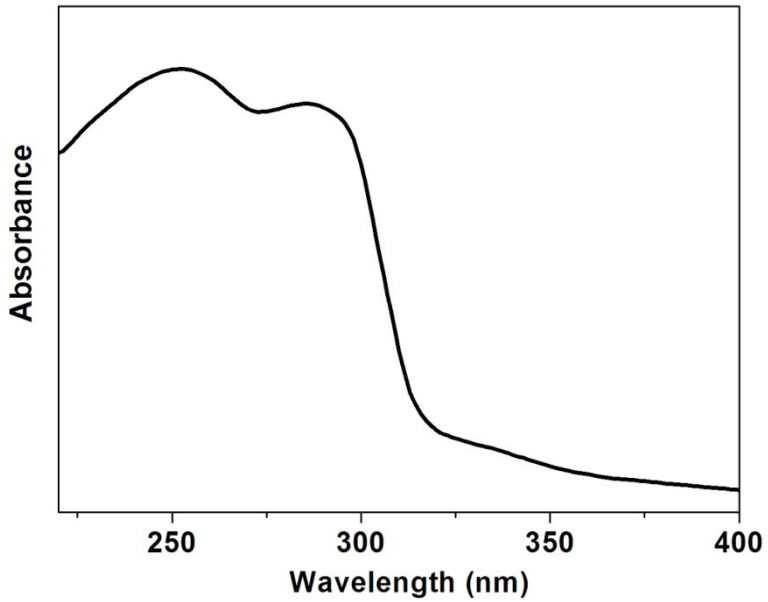

Fig. S8 The UV-vis absorption of **1** in solid state at room temperature.

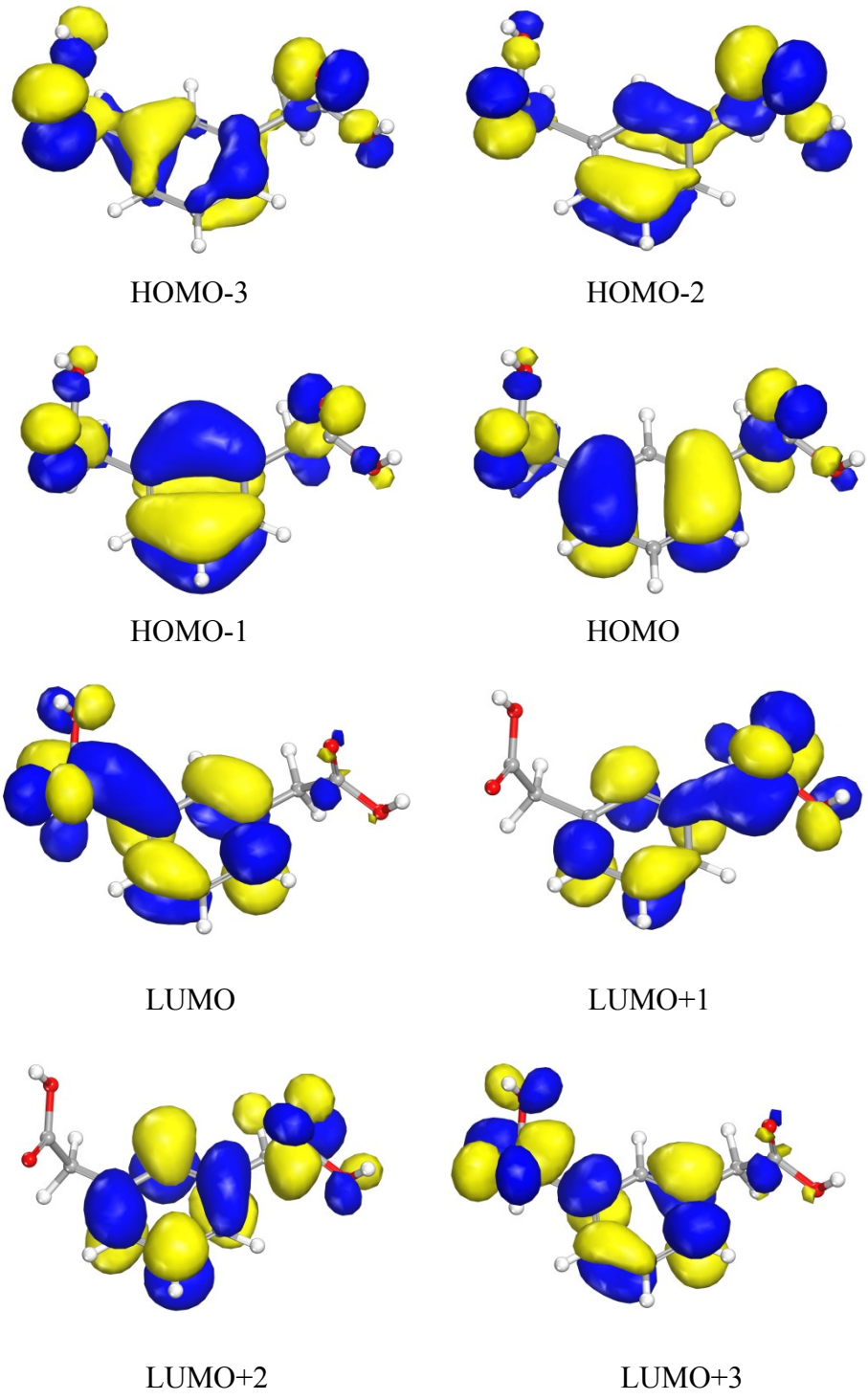

Fig. S9 The distributions of highest occupied molecular orbitals (HOMOs) and lowest unoccupied molecular orbitals (LUMOs) of free mpda.

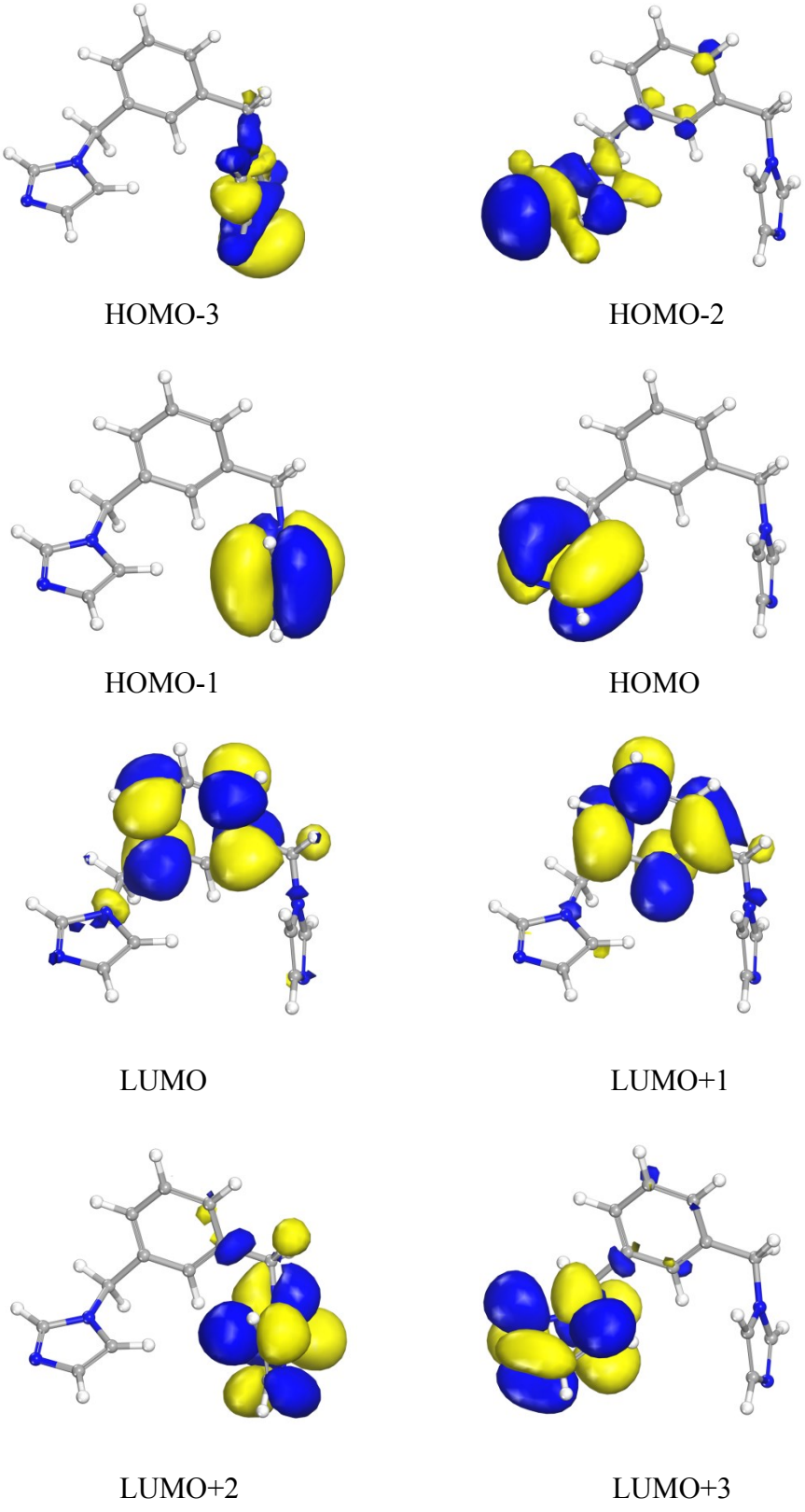

Fig. S10 The distributions of highest occupied molecular orbitals (HOMOs) and lowest unoccupied molecular orbitals (LUMOs) of free mbiyb.

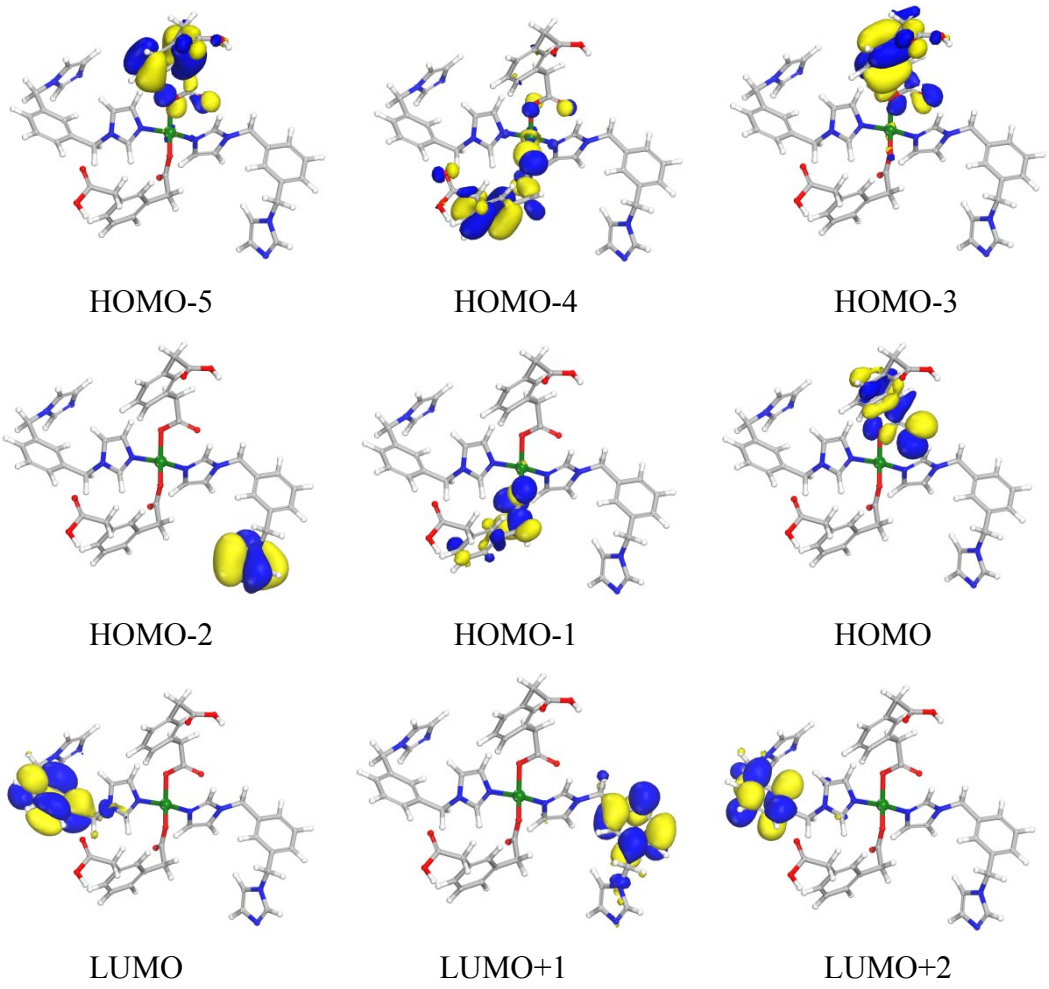

Fig. S11 The distributions of highest occupied molecular orbitals (HOMOs) and lowest unoccupied molecular orbitals (LUMOs) of **1**.

3. Supporting Table

Table S1. Crystallographic data for **1**.

MOF	**1**
Formula	$C_{24}H_{22}ZnN_4O_4$
Mass	495.82
Crystal system	Orthorhombic
Space group	$P2_12_12_1$
a (Å)	8.3124(11)
b (Å)	14.5576(19)
c (Å)	17.939(2)
α (°)	90
β (°)	90
γ (°)	90
V (Å^3)	2170.8(5)
Z	4
Dc (g cm^{-3})	1.517
μ (mm^{-1})	1.172
R_{int}	0.0196
Goof	1.045
$R_1{}^a$ / $wR_2{}^b$ *[I >2σ(I)]*	0.0265/0.0580
$R_1{}^a$ / $wR_2{}^b$ *(all data)*	0.0323/0.0670

$^aR_1 = \Sigma||F_o| - |F_c||/\Sigma|F_o|$, $wR_2 = [\Sigma w(F_o^2 - F_c^2)^2/\Sigma w(F_o^2)^2]^{1/2}$

4. Supporting References

1 (*a*) G. M. Sheldrick, *Acta Crystallogr. Sect. A*, 2008, **A64**, 112–122; (*b*) G. M. Sheldrick, *Acta Cryst*., 2015, **A71**, 3–8.

2 (*a*) B. Delley, *J. Chem. Phys*., 1990, **92**, 508–517; (*b*) B. Delley, *J. Chem. Phys*., 2000, **113**, 7756–7764; (*c*) Dmol^3 Module, MS Modeling, Version 2.2; Accelrys Inc.: San, Diego, 2003; (*d*) J. P. Perdew, J. A. Chevary, S. H. Vosko, K. A. Jackson, M. R. Pederson, D. J. Singh and C. Fiolhais, *Phys. Rev. B*, 1992, **46**, 6671–6687.